Profiling of proteins and targeting of myeloid mechanisms in atherosclerosis

Delfos, L.

Chapter 3

Treatment with APAC, a dual AntiPlatelet AntiCoagulant heparin proteoglycan mimetic, limits early collar-induced carotid atherosclerotic plaque development in *Apoe*$^{-/-}$ mice

Ilze Bot[1], Lucie Delfos[1], Esmeralda Hemme[1], Mireia N.A. Bernabé Kleijn[1], Peter J. van Santbrink[1], Amanda C. Foks[1], Petri T. Kovanen[2], Annukka Jouppila[3,4], Riitta Lassila[4,5,6]

[1]Division of BioTherapeutics, Leiden Academic Centre for Drug Research, Leiden University, Leiden, The Netherlands

[2]Wihuri Research Institute, Helsinki, Finland

[3]Clinical Research Institute HUCH, Helsinki, Finland

[4]Research Program Unit in Systems Oncology, Medical Faculty, University of Helsinki, Helsinki, Finland

[5]Aplagon Ltd, Helsinki, Finland

[6]Coagulation Disorders Unit, Helsinki University Central Hospital, Helsinki, Finland

Short title: *APAC in atherosclerosis*

Published in Atherosclerosis 2024;397:118567

Abstract

Background and aim: Mast cell-derived heparin proteoglycans (HEP-PG) can be mimicked by bioconjugates carrying antithrombotic and anti-inflammatory properties. The dual antiplatelet and anticoagulant (APAC) construct administered, either locally or intravenously (i.v.), targets activated endothelium, its adhesion molecules, and subendothelial matrix proteins, all relevant in atherogenesis. We hypothesized that APAC influences cellular interactions in atherosclerotic lesion development and studied APAC treatment during the initiation and progression of experimental atherosclerosis.

Methods: Male western-type diet-fed *Apoe*$^{-/-}$ mice were equipped with perivascular carotid artery collars to induce local atherosclerosis. In this model, mRNA expression of adhesion molecules including ICAM-1, VCAM-1, P-Selectin, and Platelet Factor 4 (PF4) are upregulated upon lesion development. From day 1 (prevention) or from 2.5 weeks after lesion initiation (treatment), mice were administered 0.2 mg/kg APAC i.v. or control vehicle three times weekly for 2.5 weeks. At week 5 after collar placement, mice were sacrificed, and lesion morphology was microscopically assessed.

Results: APAC treatment did not affect body weight or plasma total cholesterol levels during the experiments. In the prevention setting, APAC reduced carotid artery plaque size and volume by over 50%, aligning with decreased plaque macrophage area and collagen content. During the treatment setting, APAC reduced macrophage accumulation and necrotic core content, and improved markers of plaque stability.

Conclusion: APAC effectively reduced early atherosclerotic lesion development and improved markers of plaque inflammation in advanced atherosclerosis. Thus, APAC may have potential to alleviate the progression of atherosclerosis.

Keywords: Atherosclerosis, inflammation, heparin proteoglycans, animal model, plaque stability

Introduction

Atherosclerosis, characterized by the build-up of cholesterol-containing inflammatory plaques in the arterial wall, is the main underlying pathology of acute cardiovascular events, such as myocardial infarction and stroke [1]. The atherothrombotic events occur upon inflamed or erupted endothelium, and ruptured plaques expose deeper thrombogenic layers of the plaques containing collagen and tissue factor [2]. Plaque formation is caused by the influx of lipids and inflammatory cells into the subendothelial space upon repeated endothelial damage, and it is associated with smooth muscle cell proliferation, events which gradually increase upon aging. The thrombogenic hypothesis of Duguid in 1960 was based on the discovery of mural thrombi becoming incorporated in the intima to form layered fibrous thickenings [3]. Extravasated blood may also carry blood cells, including platelets, plasma proteins, and lipids from vasa vasorum into the atheromatous foci. Later, this hypothesis was complemented by the concept of inflammation being a fundamental element of atherosclerosis [4,5]. Indeed, the all-encompassing concept of thrombo-inflammation currently dominates our understanding of this chronically progressing disease with thrombosis contributing throughout the evolution of the disease process, i.e., from the lesion initiation up to the formation of a non-occluding or occluding arterial thrombus [5,6].

The mast cell, an immune cell type involved in host defense responses and in allergic diseases and asthma, has also been shown to accumulate in advanced human atherosclerotic plaques [7,8]. In the plaque, mast cells can influence the ongoing disease process by secreting proteases and pro-inflammatory cytokines into their microenvironment [9]. However, mast cells are also the major source of heparin proteoglycans (HEP-PGs) [10]. In the vascular wall, the mast cell-derived HEP-PGs can act as local anticoagulants and may counteract the procoagulant effects upon damage. Importantly, *in vitro* experiments have revealed that the HEP-PGs released by stimulated mast cells are capable of inhibiting collagen-induced platelet aggregation uniquely from other agonists. Also, perfusion of blood, spiked with isolated HEP-PG, over a collagen surface inhibits the growth of the platelet-rich thrombus under the high-shear rate and von Willebrand factor (VWF)-mediated conditions [11,12]. HEP-PGs are, thus, antithrombotic both when they are immobilized on collagen surface or when they are present in the blood [11,13]. Importantly, locally applied isolated HEP-PG was shown to inhibit thrombus formation at microsurgical anastomosis sites *in vivo* [14].

Based on the antithrombotic properties of HEP-PGs, we have tailored a semisynthetic bioconjugate with a standardized number of heparin chains onto human serum albumin. This bioconjugate exhibits both antiplatelet and anticoagulant activity (APAC) [15], and it so alleviates ischemic reperfusion injury (IRI) in the kidneys [16], brain [17] and the heart (unpublished data). Due to their rapid targeting to the injured vasculature [18] and small dosing, the APAC conjugates have initially been designed as local antithrombotics for surgical and other intervention strategies to avoid bleeding complications. Importantly, in these settings the primary hemostasis is preserved and several platelet-agonist routes function normally.

Interestingly, APAC was found to be capable of attenuating vascular injury and immune cell activation in a rat model of ischemia-reperfusion induced acute kidney injury [16]. With vascular injury and immune activation being important triggers and promoters of atherogenesis, the above data suggest that APAC may alleviate the progression of atherosclerosis. Other antithrombotic agents have shown a protective profile in animal models of atherosclerosis, which supports this hypothesis. In two independent studies, treatment with rivaroxaban, a factor Xa inhibitor, demonstrated plaque-stabilizing effects in Apolipoprotein E-deficient (*Apoe*$^{-/-}$) mice, by increasing cap thickness [19], and by reducing macrophage and necrotic core content [20]. In clinical use, rivaroxaban, when combined with aspirin to reach inhibition of activity of both coagulation Factor Xa and thromboxane-stimulated platelets, benefitted some patients having severe atherosclerotic peripheral arterial occlusive disease (COMPASS trial) [21].

Our study aimed at assessing the effects of APAC treatment both during initial (prevention setting) and progressing (treatment setting) atherosclerosis in an *Apoe*$^{-/-}$ mouse model with collar-induced lesions, where local hemodynamic alterations play a significant role.

Materials and methods

APAC

APAC, a semisynthetic highly polyanionic bioconjugate of unfractionated heparin (UFH) (7 ± 2 chains, MW appr. 180 kDa) to albumin core was provided by Aplagon Ltd. The APAC complex was characterized by polyacrylamide gel electrophoresis (PAGE; Tris-Glycine 4-20%, Mini-Protean TGX gel, Bio-Rad, Hercules, CA, USA; 120 V for 15 min and 45 min 180 V for 45 min) under native conditions and compared with unconjugated UFH (Leo Pharma, Ballerup, Denmark), human serum albumin (Biotest AG, Dreieich, Germany), and MW standard (st) (MWP04, Nippon Genetics Europe, Düren, Germany). The gel was stained sequentially with 0.125 % Alcian Blue 8GX (Sigma-Aldrich, Merck KGaA, Darmstadt, Germany) in 25% EtOH, 10% HAc, and Bio-Safe Coomassie Brilliant Blue G-250 (Bio-Rad) to detect glycosaminoglycan and protein moieties, respectively.

Animals

All animal experiments were performed in compliance with the guidelines of the Dutch government and the Directive 2010/63/EU of the European Parliament. The experiments were approved by the Ethics Committee for Animal Experiments and the Animal Welfare Body of Leiden University (Project 106002017887), and executed in compliance with the ARRIVE guidelines, taking the 3R principles into account. The outlines of the prevention and treatment setting of the experiments are provided in Supplemental Figure 1.

Ten to twelve-week-old male *Apoe*$^{-/-}$ mice on a C57BL/6 background (n=14-15/group) were bred in-house and provided with food and water ad libitum. The mice were fed a cholesterol-rich Western-type diet (0.25% cholesterol, 15% cocoa butter, Special Diet Services, Essex, UK), from 2 weeks before (T=-2 weeks) up to 5 weeks after collar placement. At week 0, the mice were randomized into groups based on age, weight, and serum cholesterol levels. Carotid artery plaque formation was induced by bilateral perivascular collar placement in these mice, as described previously [22]. This collar model has previously been shown to provide established atherosclerosis in male hyperlipidemic mice [22]. In this model, mRNA expression of adhesion molecules including ICAM-1, VCAM-1, P-Selectin, and Platelet Factor 4 (PF4) are upregulated upon lesion development, rendering this model highly suitable for our research question.

In short, mice were anesthetized by subcutaneous injection of ketamine (60 mg/kg), fentanyl citrate, and fluanisone (1.26 mg/kg and 2 mg/kg, respectively), after which sedation was monitored by toe pinch. Access to the anterior cervical triangles was gained through a sagittal anterior neck incision and both carotid arteries were carefully dissected free from the surrounding tissue. Silastic collars (Dow Corning) were placed around both carotid arteries and fixed with 3 circumferential silk ties. Subsequently, the entry wound was closed, and the animals were returned to their cage for recovery from anesthesia.

Immediately (initiation) or from week 2.5 weeks (progression) after the collar placement onwards, the mice received either 0.2 mg/kg APAC (Aplagon Ltd, Helsinki, Finland), or vehicle (137 mM NaCl, 10 mM Na_2HPO_4, pH7.5) as control three times per week via intravenous (i.v.) injection into the tail vein for 2.5 weeks (n=12-14 per group due to some loss of animals after surgery). This dose of APAC was chosen based on earlier observations upon repeated dosing of APAC as described by Craige et al. [23] and own unpublished data. The administered APAC dose (0.2 mg/kg i.v.) was adjusted according to the heparin glycosaminoglycan (GAG) content as defined by a Blyscan Sulfated Glycosaminoglycan Assay (Biocolor Ltd., Carrickfergus, Northern Ireland, UK), and a reference curve for UFH. Blood was collected from the tail vein in weeks 2 and 3. At week 5, the mice were sacrificed upon subcutaneous administration of anesthetics (ketamine (100 mg/kg) and xylazine (10 mg/kg)). Blood was collected via the orbital route, and thereafter the mice were perfused with PBS through the left cardiac ventricle. Upon complete PBS perfusion, organs were collected for analysis. Supplementary Figure 1 illustrates the administration strategy for this study with the two experimental settings; the prevention and treatment models.

Cholesterol Assay

Serum was collected after centrifugation of blood at 8000 rpm for 10 minutes at 4˚C and stored at -80˚C until analysis. Total cholesterol levels were determined through an enzymatic colorimetric assay (Roche/Hitachi, Mannheim, Germany). Precipath standardized serum (Roche Diagnostics) was used as an internal standard.

Cell Isolation and Analysis

For general white blood cell analysis, blood samples were lysed with ACK lysis buffer (0.15 M NH_4Cl, 1 mM $KHCO_3$, 0.1 mM Na_2EDTA, pH 7.3) to obtain a single white blood cell suspension. These were extracellularly stained with a mixture of selected fluorescently labeled antibodies (Supplementary Table 1) for 30 minutes at 4˚C.

Whole blood samples were collected in citrate-coated tubes and gently mixed with prewarmed PBS (1:1). The whole blood samples were stained with fluorescently labeled antibodies for 15 min at room temperature. Single-cell and whole blood samples were measured with a Cytoflex S (Beckman and Coulter, USA) and analyzed with FlowJo v10.7 (Treestar, San Carlos, CA, USA).

Histology

After euthanasia, the carotid arteries were dissected, embedded, and frozen in Tissue-Tek OCT compound (Sakura Finetek USA, Inc., Torrance CA, USA). Subsequently, 10 μm sections of

the carotid arteries were prepared for histological analysis. For each artery, collection of the sections started immediately on the proximal side of the collar, and for each slide, the sections were collected every 90 μm until the complete disappearance of the plaque. This strategy also covers the hemodynamical impact of blood-vessel wall interphase upon the atherosclerotic lesions. Mean plaque size, plaque size at the site of maximal stenosis, plaque volume, and necrotic areas were measured using hematoxylin and eosin (H&E) staining. The collagen content of the plaque was measured using a Sirius Red staining. Macrophage content was determined by using MOMA-2 antibody (1:1000; rat IgG2b; Bio-Rad). Vascular smooth muscle cells were stained using an α-smooth muscle actin antibody (1:1000, IgG2a, Sigma). Mast cells and neutrophils were manually counted after staining slides using a Naphthol AS-D Chloroacetate Specific Esterase Kit (Sigma). All slides were analyzed with a Leica DM-RE microscope and LeicaQwin software (Leica Imaging Systems).

RNA isolation, cDNA synthesis, and qPCR

Three to four carotid artery plaque segments, obtained at 5 weeks after collar placement, were pooled and homogenized in guanidine thiocyanate (GTC) using as tissue homogenizer, after which total RNA was extracted (n=4 samples per group). RNA was reverse transcribed by M-MuLV reverse transcriptase (RevertAid, MBI Fermentas). Quantitative analysis of genes (Supplementary Table 2) was performed with a 7500 fast real-time PCR system (Applied Biosystems).

Plasma coagulation times

Prior to the atherosclerosis studies, *Apoe*$^{-/-}$ mice (n=3/group) administered with 0.2 mg/kg APAC, 0.2 mg/kg unfractionated heparin (UFH), or vehicle and blood was collected by retro-orbital bleeding at 15 min after dosing. Activated partial thromboplastin time (APTT) (SynthaSIL, IL Werfen, Germany) and thrombin time (TT) (STA Thrombin2, Stago, France) were assessed from citrated (3.2%) plasma obtained after centrifugation (8000 rpm).

Statistical analysis

Data were analyzed using Prism 9.0 (GraphPad Software, Inc. San Diego, CA, USA), and are expressed as mean ± SEM for all analyses. The Shapiro-Wilkson normality test was used to test data for normal distribution. Normally distributed data were compared with an unpaired two-tailed Student t-test. When data were not normally distributed, a Mann-Whitney U test was used. Probability values of $p<0.05$ were considered significant.

Results

The APAC conjugation reaction was characterized by PAGE analysis under non-reducing conditions. Non-conjugated UFH and HSA showed distinct migration patterns in comparison with APAC and in relation to molecular weight standards (Figure 1). APAC effects on plasma coagulation times were assessed separately from the main study in *Apoe*$^{-/-}$ mice administered with 0.2 mg/kg of APAC, UFH, or vehicle. Neither APAC nor UFH, after a single intravenous administration at this concentration, affected plasma coagulation times in the *Apoe*$^{-/-}$ mice (Supplementary Figure 2).

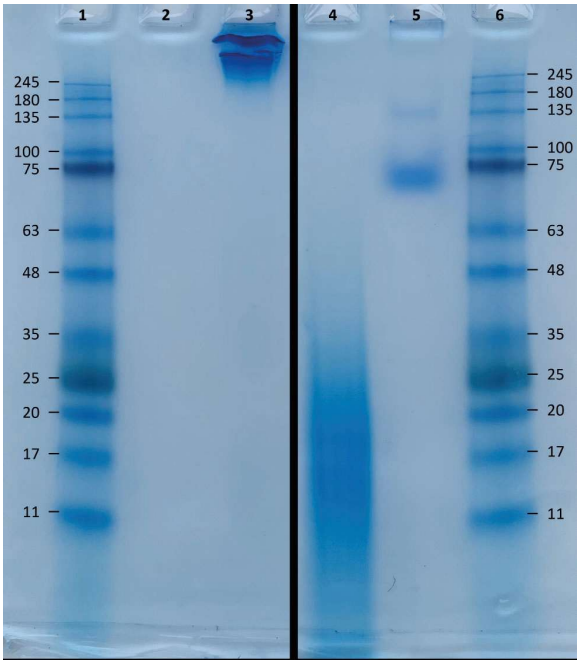

Figure 1. APAC is a bioconjugate between HSA and UFH. Conjugation of UFH chains to HSA in APAC is depicted by PAGE analysis under native, non-reducing, conditions: 1. and 6. MW st, 2. PBS buffer control, 3. APAC (4 µg; the heparin equivalent quantity), 4. UFH (5 µg), and 5. HSA (2 µg). Tris-Glycine 4-20% gel, stained with Alcian Blue and Coomassie Brilliant Blue to detect glycosaminoglycan and protein moieties, respectively.

APAC prevents early development of atherosclerosis

In the prevention setup, we assessed the effects of APAC administration (0.2 mg/kg i.v.) on the initial lesion induction and development. APAC was administered immediately after placement of the collar to induce atherosclerosis in *Apoe*$^{-/-}$ mice (Supplementary Figure 1). APAC did not affect total body weight or plasma total cholesterol levels during the study (Supplementary Figure 3A, B). Also, APAC treatment during the first 2.5 weeks of lesion development did not influence the percentage of circulating myeloid populations, including monocytes and neutrophils (Supplementary Figure 3C, D), or the B and T lymphocytes (Supplementary Figure 3E, F, G) at the endpoint of the study.

Administration of APAC during lesion initiation reduced plaque development (p<0.01) at the sites of maximal stenosis: the size of the plaques was more than 50% smaller compared to the control group (Figure 2A, B). This observation was also translated into a smaller average lesion size throughout the collar-induced plaque (Figure 2C, D, p<0.01). Consequently, the total plaque volume was diminished by 60% (p<0.05, Figure 2E) in the APAC-treated mice. The medial layer was not impacted by APAC at the site of maximal stenosis (Figure 2F), but the total vessel area was significantly inhibited by APAC treatment (control: 1.6 ±0.1*10^5 µm^2 versus APAC: 1.2±0.1*10^5 µm^2, p<0.05, Figure 2G), suggesting that APAC treatment prevented outward remodeling to a certain extent.

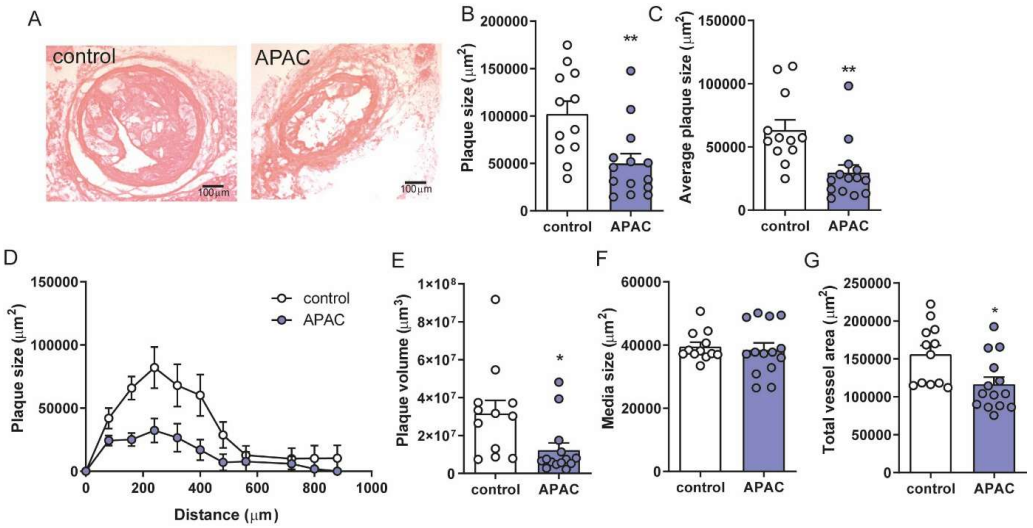

Figure 2. In the prevention setting APAC inhibits atherosclerotic lesion initiation. (A) Representative H&E staining images of collar-induced atherosclerotic plaques observed in control and APAC-treated *Apoe*$^{-/-}$ mice. (B) APAC reduced collar-induced atherosclerosis at the site of maximal stenosis. (C) APAC reduced the average sizes of the lesions over 50%. (D) Distance analysis revealed smaller atherosclerotic lesions in the APAC-treated mice than in the controls throughout the carotid artery plaque, resulting in (E) a strong reduction in plaque volume. (F)

Media size did not differ between the APAC and control groups. (G) Total vessel area at the site of maximal stenosis was reduced upon APAC treatment. N=12-14, data are given as mean±SEM. *p<0.05, **p<0.01.

Further analysis of plaque morphology revealed that the average macrophage areas in the plaques tended to reduce upon APAC treatment (p=0.05, Figure 3A, B), while the macrophage content relative to lesion size remained unchanged (Figure 3C). Similarly, both absolute collagen (p<0.01, Figure 3D-F) and necrotic areas (p<0.05, Figure 3G, H) were decreased in the APAC-treated mice versus controls significantly by over 50%. Vascular smooth muscle cell content, both absolute and relative to lesion size, did not differ between the groups (Supplementary Figure 4A, B). As the values relative to lesion size were not altered, our data suggest that lesions in the APAC treated group represent an earlier stage of development than in the control plaques, and that APAC thus inhibited overall lesion development. APAC treatment did not influence the mast cell numbers or its activation status in the perivascular tissue (Figure 3I). In addition, the numbers of neutrophils in the intima seemed somewhat, but not significantly, reduced (Figure 3J).

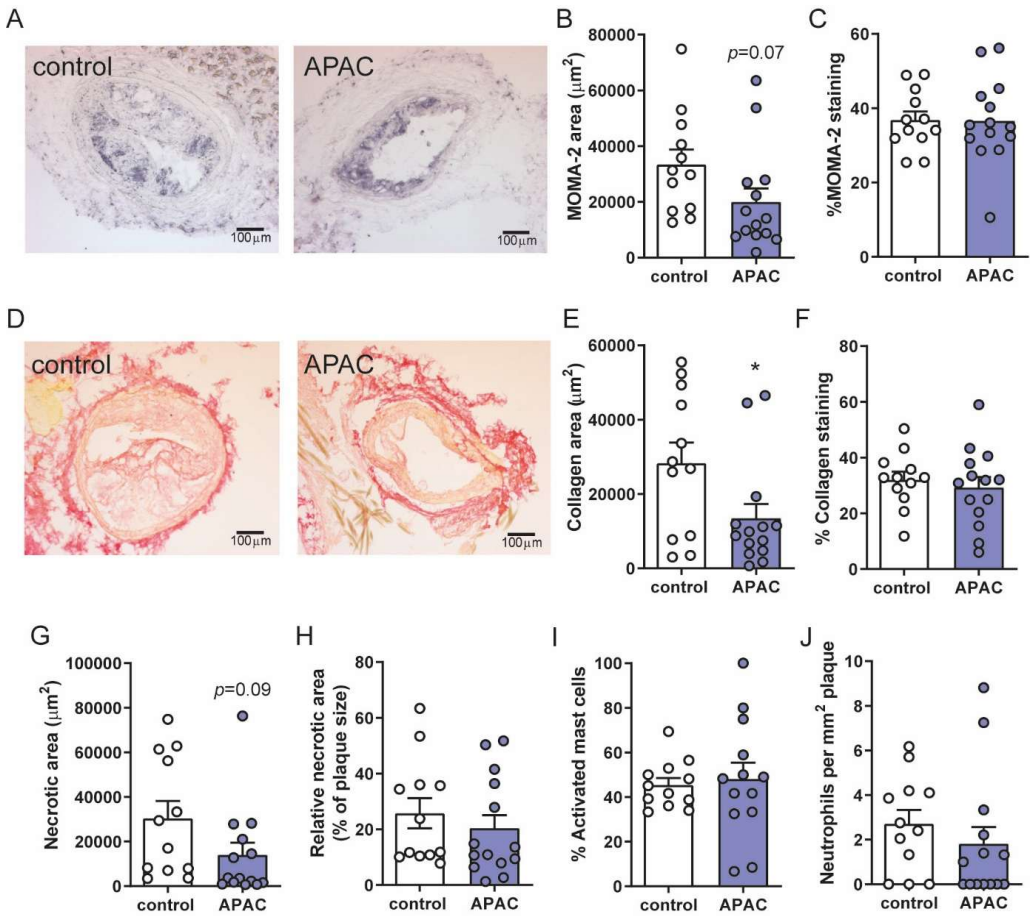

Figure 3. Plaque morphology analysis in the APAC prevention setting. (A) Representative images of MOMA-2 staining, showing macrophage positive areas in the carotid artery plaques. (B) Absolute macrophage area tended to be reduced upon APAC treatment compared to controls. (C) Relative to plaque size, macrophage content did

not differ between the groups. (D) Collagen content in the carotid artery plaques was measured using a Sirius Red staining, of which representative images of the control and APAC groups are displayed. (E) Absolute collagen area was significantly smaller in plaques of the APAC-treated mice compared to controls, (F) while the collagen content relative to lesion size was similar between the groups. APAC tended to reduce the necrotic core area of the plaque both in the absolute (G) and relative (H) values. (I) Percentage of activated mast cells in the perivascular tissue. (J) Neutrophil numbers in the plaque. N=12-14, data are given as mean±SEM. *p<0.05.

APAC reduces markers of inflammation in advanced plaques

In the treatment set-up, we aimed to assess the effects of APAC treatment on the progression of the already developing atherosclerotic lesions at 2.5 weeks after the initiation of collar-accelerated carotid artery atherosclerosis (Supplementary Figure 1). As in the previous experiments, APAC did not influence total body weight or plasma total cholesterol levels (Supplementary Figure 5A, B). Circulating white blood cell and total platelet counts remained unaffected as well (Supplementary Figure 5C-G).

Treatment with APAC upon lesion progression did not significantly affect the carotid plaque size at the site of maximal stenosis (Figure 4A, B). Also, the average lesion size throughout the carotid artery plaque did not significantly differ between the groups (Figure 4C). APAC-treated lesions tended to progress less along with increasing distance from the collar placement (Figure 4D). Indeed, plaque volume tended to be decreased, although not significantly, in the APAC-treated group (p=0.1, Figure 4E), and so did the average plaque length when expressed in the distance proximal from the collar (p=0.07, Figure 4F). In the treatment setting, APAC treatment did not impact either the surface area of the medial layer (Figure 4G) or total vessel area (control: $1.4\pm0.2*10^5$ μm^2 versus APAC: $1.3\pm0.1*10^5$ μm^2, Figure 4H) at the site of maximal stenosis.

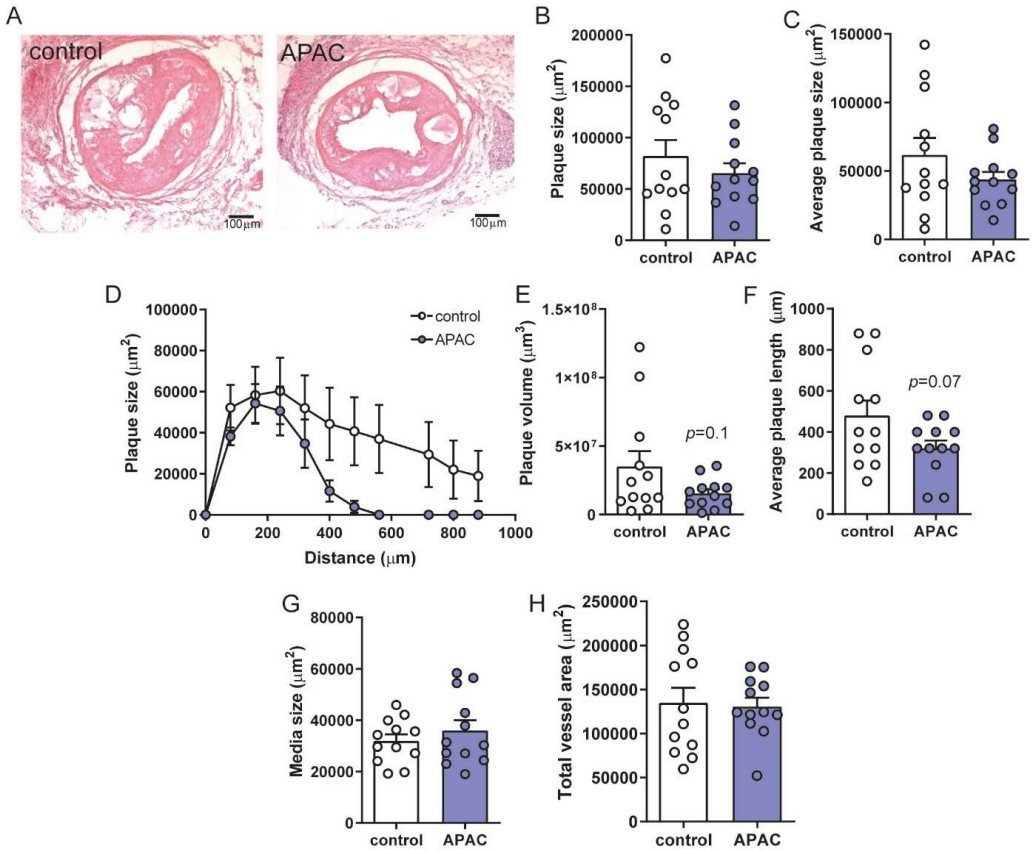

Figure 4. In the treatment setting APAC attenuated atherosclerosis progression. (A) Representative H&E staining images of collar-induced atherosclerotic plaques observed in control and APAC-treated *Apoe*$^{-/-}$ mice during lesion progression. (B) APAC treatment during lesion progression did not affect collar-induced atherosclerosis at the site of maximal stenosis or on (C) average lesion size level. (D) Distance analysis revealed a tendency to smaller atherosclerotic surface area in the APAC group compared to the controls when the distance from the collar increased. (E) Plaque volume was not significantly reduced, however, in (F), the average plaque length tended to be reduced upon APAC treatment. (G) Media thickness and (H) Total vessel area did not differ between the APAC and the control group. N=12-14, data are given individually and as mean±SEM. N=12-14 per group, data are given as mean±SEM.

However, interestingly, macrophage area was significantly reduced with 42% in the APAC-treated group (p<0.05, Figure 5A-C). While the collagen content was unaffected (Figure 5D-F), the absolute necrotic core size tended to reduce (p=0.07, Figure 5G). As in the prevention setting, APAC treatment did not affect smooth muscle cell content (Supplementary Figure 6A, B). Relative to the lesion size, the necrotic area diminished by 25% (p<0.05, Figure 5H). An increased collagen/necrotic area-ratio (APAC: 0.85 ± 0.06 versus 0.57 ± 0.07, p<0.01, Figure 5I) suggests that, overall, APAC treatment improved markers of plaque stability upon lesion progression. The reduction in macrophage content coincided in particular with reduced relative *Tnfα* mRNA expression levels in the carotid artery plaque (relative expression; control: 8±2*10^{-3} versus APAC: 4±2*10^{-3}, p<0.05, Figure 5J), illustrative of reduced inflammatory signaling

via TNFα. The gene expression of other inflammatory cytokines such as *Ccl2*, *Il-1β* and *Il-6* were not affected by APAC treatment (Supplementary Table 3). In addition, carotid plaque gene expression analysis of phenotypic macrophage markers such as *Ccr2*, *Mrc1* or *Arg1* did not reveal differences, suggesting that APAC did not influence the macrophage phenotype (Supplementary Table 3). Along the prevention setting, neither the activation status of perivascular mast cells (Figure 5K) nor the neutrophil numbers (Figure 5L) differed between the groups.

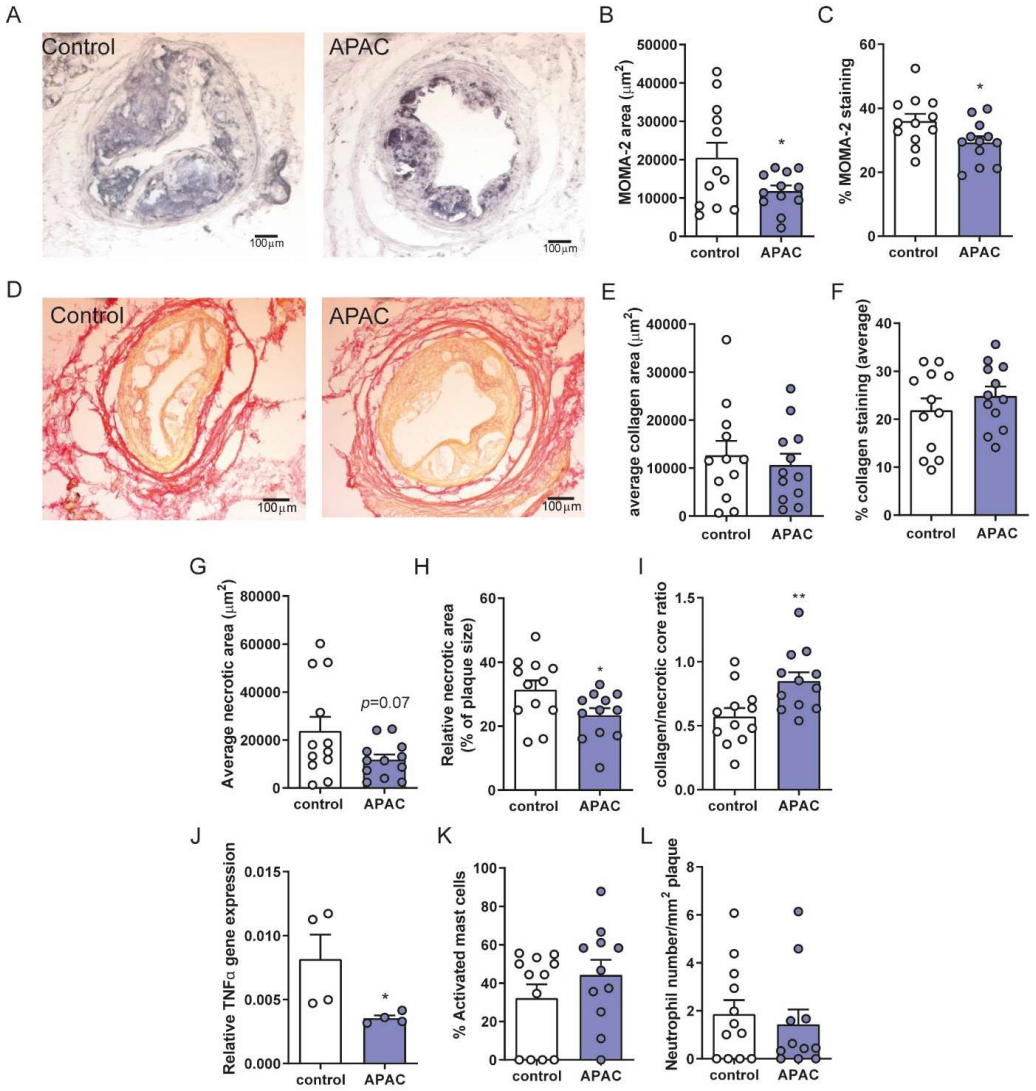

Figure 5. Plaque morphology analysis in the APAC treatment setting. (A) Representative images of MOMA-2 staining show macrophage-positive areas in the carotid collar-induced atherosclerosis in both groups. Macrophage content was significantly reduced by APAC treatment compared to controls, both in the absolute area (B) and (C) relative to the plaque size. (D) Collagen content of the carotid artery plaques was analyzed using a Sirius Red staining, and representative images of the control and APAC groups are shown. (E) Absolute collagen area did not differ between plaques of the APAC-treated mice and the controls, and the content relative to lesion size was also similar (F). The necrotic core area of the plaque was reduced in the absolute values (G), which were significant

relative to lesion size (H). (I) The collagen/necrotic core ratio was significantly increased in the APAC group. (J) Relative TNFα gene levels in pooled carotid artery plaques. (K) Percentage of activated mast cells in the perivascular tissue and (L) Neutrophil numbers in the plaque were similar. N=12-14, data are given as mean±SEM. *p<0.05, **P<0.01.

Discussion

In the present study, we aimed to assess the efficacy of APAC, a potent antiplatelet and anticoagulant treatment modality, in the inhibition of atherosclerotic lesion development and progression in a mouse model, in which the endothelium is activated due to the presence of hyperlipidemia and increased oscillatory shear stress [22]. First, we confirmed that APAC indeed is a heparin-proteoglycan mimetic, based on the bioconjugation between the UFH chains to HSA core. *In vivo*, we showed that APAC reduced initial atherosclerotic lesion formation and limited inflammation in pre-existing lesions in a therapeutic setting, independently of plasma cholesterol levels, as summarized in Figure 6. As local thrombotic responses and inflammation are seminal pathogenic features in tissue injury and atherogenesis [1,4,5], the present findings support the vascular reprogramming potential of APAC in these pathological processes.

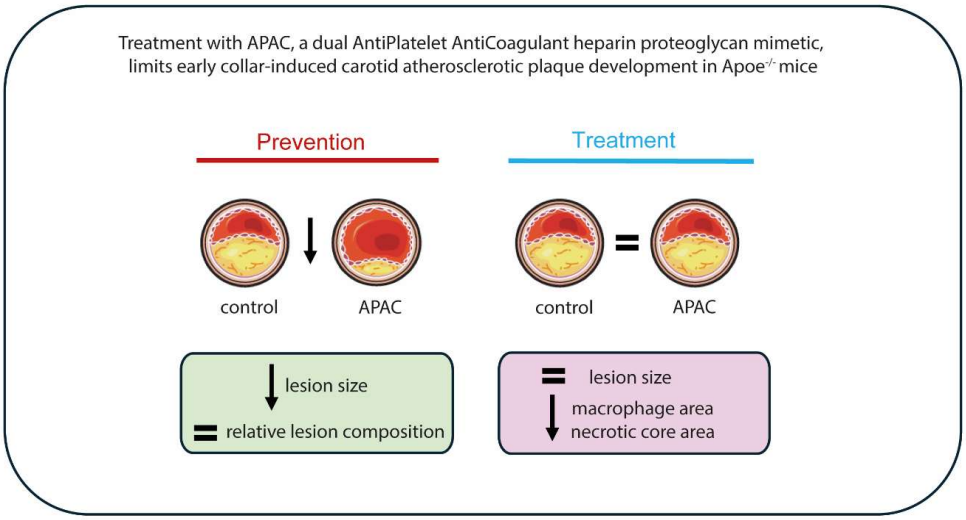

Figure 6. Graphical abstract with a summary of the main study findings.

In models of arterial injury triggered by balloon angioplasty and arteriovenous fistula surgery, we have previously shown that local APAC administration colocalizes with VWF, collagen, and laminin in areas with endothelial loss [18]. Also, in mice subjected to a laser-induced carotid injury, the arterial occlusion time was prolonged by APAC in comparison with UFH, and in a collagen-exposing carotid surgery model, APAC rapidly binds to the extracellular matrix, and upon such binding the platelet thrombus formation is practically abolished [24]. In an IRI model of kidney injury in rats [16] and in myocardial injury in mice (unpublished), a single intravenously administered dose of APAC (0.13 or 0.5 mg/kg, respectively) has shown strong tissue-protective and anti-inflammatory properties. Therefore, the unique and multifunctional properties of APAC, including the targeting and binding to arterial injury sites

and the preservation of its functionality *in situ,* render this compound capable of locally attenuating platelet-collagen interactions, and thrombin and fibrin formation at the injured tissue locations [15,18,24,25]. In the current study, we now also firmly establish that APAC protects against early atherosclerosis development which is reflected by the presence of plaques with a less advanced phenotype. In more advanced lesions, plaque inflammation was limited by APAC, as illustrated mainly by a reduced macrophage content as well as by the reduced size of the necrotic core.

We did not observe prolongation of APTT or thrombin time after a single intravenous injection with either APAC or UFH in *Apoe*$^{-/-}$ plasma, unlike previously in normal mouse plasma [23]. Although APTT and TT after repeated APAC administration remain to be assessed in our mouse model, hyperlipidemia in humans is associated with enhanced thrombin generation [26], which may explain the lack of effect in our hyperlipidemic mice. The underlying mechanisms via which APAC protects against lesion initiation and stabilizes more established lesions remain to be better understood, although previous studies using anticoagulants have provided evidence for anti-inflammatory pathways also to be involved. For example, as has been described for the FXa inhibitor rivaroxaban [19,20], we observed reduced plaque inflammation in the prevention but most prominently in the treatment study. Also, double knock-out models of *Apoe*$^{-/-}$ and FVIII or FXI show that coagulation factors reduce the development of atherosclerosis, due to for example a reduction in plaque macrophage content [27,28]. We also demonstrated a reduced macrophage content, suggesting that APAC may inhibit the influx of pro-inflammatory monocytes into the lesion. This may occur via a reduction of the inflammatory mediators TNFα, IL-6 and MCP-1. Indeed, we observed a reduction particularly in TNFα mRNA expression in the plaques of the therapeutic study, supporting this notion at least partially. The exact underlying mechanisms that lead to the reduced inflammation remain to be investigated. Based in our gene expression analysis of the atherosclerotic plaques, there is no indication for an alteration in the macrophage phenotype by APAC treatment. We hypothesize that APAC may act anti-inflammatory via downregulation or shielding of adhesion molecules such as P-selectin and PF4. Previously, APAC has been shown, via its polyanionic charge, to have a strong binding affinity to multiple positively charged blood and extracellular matrix proteins, which are involved in progression of atherosclerosis, including VWF, neutrophil binding chemokine PF4 [29] and P-selectin [30], as has been reported also in the cancer setting. Overall, the limited influx of inflammatory cells into the vascular wall did result in a reduction in the necrotic core formation, which we observed as the most prominent APAC-dependent effect in the progression study.

We should consider the possibility that APAC, which can bind LDL-particles via ionic interaction with the positively amino-acid residues of the apoB-component of the particles, may compete with arterial proteoglycans for LDL-binding in the arterial wall. This would reduce the retention and modification of the LDL-particles in the plaque, leading to reduced foam cell formation and necrotic core formation. This is relevant when considering the pathogenesis of atherosclerosis, in which lesion formation is characterized by both extra- and intracellular

accumulation of lipids. These lipids, derived from apolipoprotein B (apoB)-containing lipoproteins that have entered the arterial intima, bind to the proteoglycan structures in the arterial wall and then become modified by oxidative agents and hydrolytic enzymes [31]. Such modified lipoprotein particles are subsequently recognized and ingested by macrophages that differentiate into foam cells, which ultimately die and participate in the formation of the necrotic lipid core [32]. Via lipoprotein retention, APAC may thus limit this process, provided it reaches the sites of endothelial activation or the subendothelial space upon increased shear stress, prevalent in our collar model.

Although we do not observe plaque rupture in our mouse model of atherosclerosis, we do not exclude local effects of APAC on atherothrombosis. This is because our data closely relate to studies investigating the role of VWF in atherogenesis. In the 1980s, Fuster et al. observed that homozygous VWF-deficient pigs were almost devoid of aortic atherosclerosis, while control pigs with normal VWF levels expressed marked atherosclerosis [33]. In another study, the involvement of VWF in atherogenesis was examined in hypercholesterolemic LDL receptor-deficient mice by breeding them with VWF-deficient mice [34]. Half of the aortic lesions were located at the branch points of the renal and mesenteric arteries where disturbed blood flow exists. Importantly, the lesions at these sites were 40% less prominent in the VWF-negative mice, quite similar to our collar-injured carotid lesions in the *Apoe*$^{-/-}$ mice. The authors suggested that VWF deficiency may have reduced platelet and leukocyte adhesion to the lesion sites and/or attenuating mechano-transduction pathways of shear forces to the endothelium in the vascular wall. These prior results coincide well with those of our earlier work, particularly since, by using human blood, we could previously demonstrate significant inhibition of high shear-induced VWF-mediated thrombus growth both with APAC and its parent molecule of heparin proteoglycans [11,25]. Closing the loop back to atherothrombosis and inflammation, the many VWF-mediated mechanisms of platelet-vessel wall interactions which involve adhesion molecules, represent therapeutic targets in the early phases of thrombo-inflammatory atherogenesis [35-39].

Altogether, as summarized in the graphical abstract, the protective features of APAC against atherothrombosis, and particularly inflammation, are likely to underlie the efficacy of APAC in experimental atherosclerosis, not only in preventive but also in treatment settings.

Conflict of interest

RL is the CSO and CMO of Aplagon Ltd. The other authors declare no competing interests.

Author contributions

Ilze Bot: conceptualization, executing experiments, data acquisition, data analysis, and interpretation, writing - original draft, funding acquisition. **Lucie Delfos**: data acquisition, data analysis, writing – review, and editing. **Esmeralda Hemme**: data acquisition, writing – review, and editing. **Mireia Bernabé Kleijn**: executing experiments, data acquisition. **Peter van Santbrink**: executing experiments, data acquisition. **Amanda Foks:** data acquisition, writing – review, and editing. **Petri Kovanen**: conceptualization, supervision, writing – review, and editing. **Annukka Jouppila:** Development of APAC, conceptualization, data analysis and interpretation, writing - original draft. **Riitta Lassila:** Invention and development of APAC, conceptualization, supervision, writing – review, and editing.

Acknowledgement

The authors would like to thank Anish Kanhai and Iris van Wissen (LACDR, Leiden University) for technical assistance.

References

[1] Libby P, Buring JE, Badimon L, Hansson GK, Deanfield J, Bittencourt MS, Tokgözoğlu L, Lewis EF. Atherosclerosis. Nat Rev Dis Primers. 2019;5:56.

[2] Taubman MB, Fallon JT, Schecter AD, Giesen P, Mendlowitz M, Fyfe BS, Marmur JD, Nemerson Y. Tissue factor in the pathogenesis of atherosclerosis. Thromb Haemost. 1997;78:200-204.

[3] Duguid JB. The thrombogenic hypothesis and its implications. Postgrad Med J. 1960;36:226-229.

[4] Jang IK, Lassila R, Fuster V. Atherogenesis and inflammation. Eur Heart J. 1993;14 Suppl K:2-6.

[5] Ross R. Atherosclerosis--an inflammatory disease. Engl J Med. 1999;340:115-126.

[6] Lassila R, Peltonen S, Lepäntalo M, Saarinen O, Kauhanen P, Manninen V. The severity of atherosclerosis is associated with fibrinogen and degradation of cross-linked fibrin. Arterioscler Thromb, 1993;13:1738-1742

[7] Kaartinen M, Penttilä A, Kovanen PT. Accumulation of activated mast cells in the shoulder region of human coronary atheroma, the predilection site of atheromatous rupture. Circulation. 1994;90:1669-1678.

[8] Willems S, Vink A, Bot I, Quax PH, de Borst GJ, de Vries JP, van de Weg SM, Moll FL, Kuiper J, Kovanen PT, de Kleijn DP, Hoefer IE, Pasterkamp G. Mast cells in human carotid atherosclerotic plaques are associated with intraplaque microvessel density and the occurrence of future cardiovascular events. Eur Heart J. 2013;34:3699-3706.

[9] Kovanen PT, Bot I. Mast cells in atherosclerotic cardiovascular disease - Activators and actions. Eur J Pharmacol. 2017;816:37-46.

[10] Hellman L, Akula S, Fu Z, Wernersson S. Mast Cell and Basophil Granule Proteases - In Vivo Targets and Function. Front Immunol. 2022;13:918305.

[11] Lassila R, Lindstedt K, Kovanen PT. Native macromolecular heparin proteoglycans exocytosed from stimulated rat serosal mast cells strongly inhibit platelet-collagen interactions. Arterioscler Thromb Vasc Biol. 1997;17:3578-3587.

[12] Kauhanen P, Kovanen PT, Lassila R. Collagen-immobilized native macromolecular heparin proteoglycans strongly inhibit platelet interactions under flowing blood. Arterioscler Thromb Vasc Biol. 2000;20:e113-e119.

[13] Kauhanen P, Kovanen PT, Reunala T, Lassila R. Effects of skin mast cells on bleeding time and coagulation activation at the site of platelet plug formation. Thromb Haemost. 1998;79:843-847.

[14] Olsson E, Asko-Seljavaara S, Lassila R. Topically administered macromolecular heparin proteoglycans effectively inhibit thrombus growth in microvascular anastomoses. Thromb Haemost. 2002;87;245-51.

[15] Lassila R, Jouppila A. Mast cell-derived heparin proteoglycans as a model for a local antithrombotic. Semin Thromb Hemost. 2014;40:837-844.

[16] Tuuminen R, Jouppila A, Salvail D, Laurent CE, Benoit MC, Syrjälä S, Helin H, Lemström K, Lassila R. Dual antiplatelet and anticoagulant APAC prevents experimental ischemia-reperfusion-induced acute kidney injury. Clin Exp Nephrol. 2017;21:436-445.

[17] Denorme, F, Frösen J, JouppilaA, Lindgren A, Resendiz-Nieves J, Manninen H, De Meyer S, Lassila R. Pretreatment with a dual AntiPlatelet and AntiCoagulant APAC reduces ischemia-reperfusion injury in a mouse model of temporary middle cerebral artery occlusion - implications for neurovascular procedures. Acta Neurochir (Wien). 2024;166:137.

[18] Barreiro KA, Tulamo R, Jouppila A, Albäck A, Lassila R. Novel Locally Acting Dual Antiplatelet and Anticoagulant (APAC) Targets Multiple Sites of Vascular Injury in an Experimental Porcine Model Eur J Vasc Endovasc Surg. 2019;58:903-911.

[19] Zhou Q, Bea F, Preusch M, Wang H, Isermann B, Shahzad K, Katus HA, Blessing E. Evaluation of plaque stability of advanced atherosclerotic lesions in apo E-deficient mice after treatment with the oral factor Xa inhibitor rivaroxaban. Mediators Inflamm. 2011;2011:432080.

[20] Posthuma JJ, Posma JJN, Schep G, Bender MMH, van Oerle R, van der Wal AC, Ten Cate H, Spronk HMH. Targeting Coagulation Factor Xa Promotes Regression of Advanced Atherosclerosis in Apolipoprotein-E Deficient Mice. Sci Rep. 2019;9:3909.

[21] Branch KRH, Probstfield JL, Bosch J, Bhatt DL, Maggioni AP, Muehlhofer E, Avezum A, Widimsky P, Connolly SJ, Yi Q, Shestakovska O, Yusuf S, Eikelboom JW. Total events and net clinical benefit of rivaroxaban and aspirin in patients with chronic coronary or peripheral artery disease: The COMPASS trial. Am Heart J. 2023;258:60-68.

[22] von der Thüsen JH, van Berkel TJ, Biessen EA. Induction of rapid atherogenesis by perivascular carotid collar placement in apolipoprotein E-deficient and low-density lipoprotein receptor-deficient mice. Circulation. 2001;103:1164-1170.

[23] Craige S, Jouppila A, Humphries B, Lassila R. Safety and Functional Pharmacokinetic Profile of APAC, a Novel Intravascular Antiplatelet and Anticoagulant. J Cardiovasc Pharmacol. 2021;78:453-462.

[24] Bonetti NR, Jouppila AJ, Saravi SSS, Cooley BC, Pasterk L, Liberale LL, Gobbato S, Lüscher TF, Camici G, Lassila RP, Beer JH. Intravenously administered APAC, a dual AntiPlatelet AntiCoagulant, targets arterial injury site to inhibit platelet thrombus formation and tissue factor activity in mice. Thromb Res. 2023; 228:163-171.

[25] Chen J, Verni CC, Jouppila A, Lassila R, and Diamond SL. Dual antiplatelet and anticoagulant (APAC) heparin proteoglycan mimetic with shear-dependent effects on platelet-collagen binding and thrombin generation, Thromb Res 2018;169:143-151.

[26] Kim JA, Kim JE, Song SH, Kim HK. Influence of blood lipids on global coagulation test results. Ann Lab Med. 2015;35:15-21.

[27] Khallou-Laschet J, Caligiuri G, Tupin E, Gaston AT, Poirier B, Groyer E, Urbain D, Maisnier-Patin S, Sarkar R, Kaveri SV, Lacroix-Desmazes S, Nicoletti A. Role of the intrinsic coagulation pathway in atherogenesis assessed in hemophilic apolipoprotein E knockout mice. Arterioscler Thromb Vasc Biol. 2005;25:e123-126.

[28] Shnerb Ganor R, Harats D, Schiby G, Gailani D, Levkovitz H, Avivi C, Tamarin I, Shaish A, Salomon O. Factor XI Deficiency Protects Against Atherogenesis in Apolipoprotein E/Factor XI Double Knockout Mice. Arterioscler Thromb Vasc Biol. 2016;36:475-481.

[29] Bakogiannis C, Sachse M, Stamatelopoulos K, Stellos K. Platelet-derived chemokines in inflammation and atherosclerosis. Cytokine. 2019;122:154157.

[30] Borsig L, Wong R, Feramisco J, Nadeau DR, Varki NM, Varki A. Heparin and cancer revisited: mechanistic connections involving platelets, P-selectin, carcinoma mucins, and tumor metastasis. Proc Natl Acad Sci U S A. 2001;98:3352-3357.

[31] Borén J, Williams KJ. The central role of arterial retention of cholesterol-rich apolipoprotein-B-containing lipoproteins in the pathogenesis of atherosclerosis: a triumph of simplicity. Curr Opin Lipidol. 2016;27:473-483.

[32] Bäck M, Yurdagul Jr A, Tabas I, Öörni K, Kovanen PT. Inflammation and its resolution in atherosclerosis: mediators and therapeutic opportunities. Nat Rev Cardiol. 2019;16:389-406.

[33] Fuster V, Griggs TR. Porcine von Willebrand disease: implications for the pathophysiology of atherosclerosis and thrombosis. Prog Hemost Thromb. 1986:8:159-183.

[34] Methia N, André P, Denis CV, Economopoulos M, Wagner DD. Localized reduction of atherosclerosis in von Willebrand factor-deficient mice. Blood. 2001;98:1424-1428.

[35] van Galen KPM, Tuinenburg A, Smeets EM, Schutgens REG. Von Willebrand factor deficiency and atherosclerosis. Blood Rev. 2012;26:189-196.

[36] Wu MD, Atkinson TM, Lindner JR. Platelets and von Willebrand factor in atherogenesis. Blood. 2017;129:1415-1419.

[37]. Shim CY, Liu YN, Atkinson T, Xie A, Foster T, Davidson BP, Treible M, Qi Y, López JA, Munday A, Ruggeri Z, Lindner JR. Molecular Imaging of Platelet-Endothelial Interactions and Endothelial von Willebrand Factor in Early and Mid-Stage Atherosclerosis. Circ Cardiovasc Imaging. 2015;8:e002765

[38] Ozawa K, Packwood W, Varlamov O, Muller M, Xie A, Wu MD, Abraham-Fan RJ, López JA, Lindner JR. Elevated LDL Cholesterol Increases Microvascular Endothelial VWF and

Thromboinflammation After Myocardial Infarction. Arterioscler Thromb Vasc Biol. 2023;43:1041-1053.

[39] Chung DW, Platten K, Ozawa K, Adili R, Pamir N, Nussdorfer F, St John A, Ling M, Le J, Harris J, Rhoads N, Wang Y, Fu X, Chen J, Fazio S, Lindner JR, López JA. Low-density lipoprotein promotes microvascular thrombosis by enhancing von Willebrand factor self-association. Blood. 2023;142:1156-1166.

Supplementary material

Supplementary tables

Supplementary Table 1: Extracellular antibody panel used for flow cytometry analysis

Antibody	Fluorochrome	Clone	Supplier
CD4	V500	RM4-5	BD Horizon
CD11b	BV605	M1/70	Biolegend
Ly6G	PerCP	1A8	Biolegend
CD115	PE	AFS98	eBioscience
CD8	PE-Dazzle	53-6.7	Biolegend
CD19	PE-Cy7	1D3	BD Biosciences
CD45	AF700	30-F11	Biolegend
CD41	PB	MWReg30	Biolegend
Fixable viability dye	eFluor780	N.A.	ThermoFisher Scientific
CD16/CD32	N.A.	93	Biolegend

Supplementary Table 2: Primers used for quantitative real-time PCR analysis. All gene expression analysis was performed using three housekeeping genes (*36B4*, *Hprt*, and *Actb*)

Gene	Forward primer (3'-5')	Reverse primer (5'-3')
36b4	ctgagtacaccttcccacttactga	cgactcttcctttgcttcagcttt
Hprt	gctggtgaaaaggacctctcgaagt	caacttgcgctcatcttaggctttgt
Actb	cttctttgcagctccttcgttgccg	aatacagcccggggagcatcgtc
Pecam1	acagaagtggaagtgtcctcccttg	cgtgcactgccttgactgtcttaag
Selp	acactcctggctctgctaagaaa	agcgttagtgaagactccgtatgt
Vcam-1	agactgaagttggctcacaattaagaag	agtagagtgcaaggagttcggg
Icam-1	gtccgcttccgctaccatcac	ggtccttgcctacttgctgcc
Tnfa	caaagggatgagaagttcccaaatggc	cactccagctgctcctccacttg
Ccl2	ctgaagccagctctctcttcctc	ggtgaatgagtagcagcaggtga
Il1b	aacgacaaaatacctgtggccttg	ccgtttttccatcttcttctttgggt
Il6	agcctggagggaggaaagggct	accgggtaagaccttgcacagcag
Ccr2	gctgcctgcaaagaccagaagag	tgccgtggatgaactgaggtaaca
Mrc1	tctagcttcatcttcgggcctttgg	tgaggatccatcttcctttggtcagc
Arg1	tggcagaggtccagaagaatgg	gtgagcatccacccaaatgacac

Supplementary Table 3: Relative gene expression in control versus APAC treated carotid artery plaques in the treatment setting (n=4, pooled samples). Gene expression is displayed relative to the average of three housekeeping genes (*36B4*, *Hprt*, and *Actb*). Data are given as mean ± SEM. **p*<0.05

Gene	**Control**	**APAC**	***p*-value**
Pecam1	0.206 ± 0.041	0.163 ± 0.055	0.43
Selp	0.105 ± 0.025	0.095 ± 0.016	0.83
Vcam-1	0.172 ± 0.046	0.162 ± 0.024	0.97
Icam-1	0.015 ± 0.002	0.010 ± 0.002	0.16
Tnfa	0.0082 ± 0.0019	0.0036 ± 0.0002	0.03*
Ccl2	0.039 ± 0.003	0.036 ± 0.002	0.42
Il1b	0.0070 ± 0.0027	0.0044 ± 0.0013	0.58
Il6	0.0015 ± 0.0006	0.0035 ± 0.0011	0.38
Ccr2	0.024 ± 0.003	0.018 ± 0.003	0.25
Mrc1	0.107 ± 0.013	0.084 ± 0.017	0.30
Arg1	0.0018 ± 0.0005	0.0007 ± 0.0003	0.10

Supplementary figures

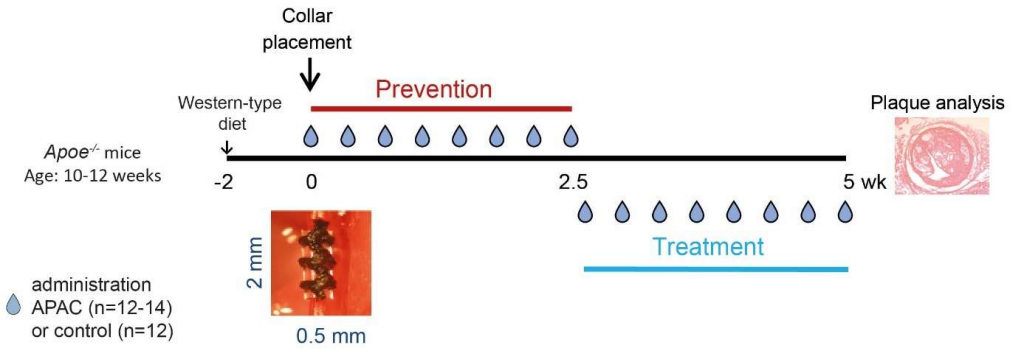

Supplementary Figure 1. Study design. The male *Apoe*$^{-/-}$ mice were fed a cholesterol-rich western-type diet from 2 weeks before up to 5 weeks after bilateral perivascular collars were placed to accelerate carotid artery atherosclerosis. APAC (0.2 mg/kg i.v.) or vehicle was administered 3 times per week for 2.5 weeks, either starting at the collar placement (prevention setting) or after 2.5 weeks (treatment setting) atherosclerosis progression. Blood was collected from the tail vein on week 2 and 3. At the study termination week 5, tissues were collected for analysis.

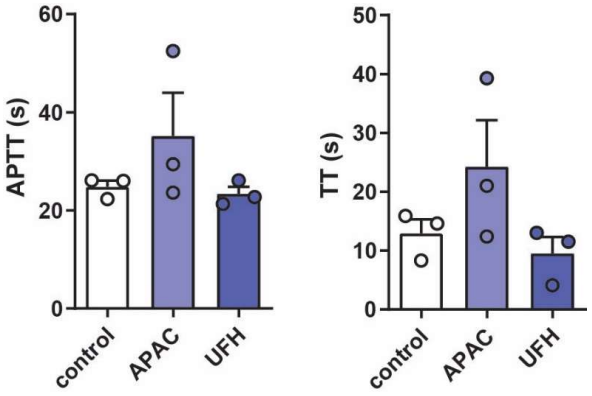

Supplementary figure 2. Coagulation times in *Apoe*$^{-/-}$ mouse plasma after a single intravenous administration of vehicle control, APAC or unfractionated heparin (UFH). A) Activated partial thromboplastin time (APTT), and B) thrombin time (TT) in *Apoe*$^{-/-}$ mouse plasma collected 15 min after a single intravenous bolus of either PBS control (CTRL), APAC (0.2 mg/kg) or UFH (0.2 mg/kg). N=3 per group, data are given as mean±SEM**.**

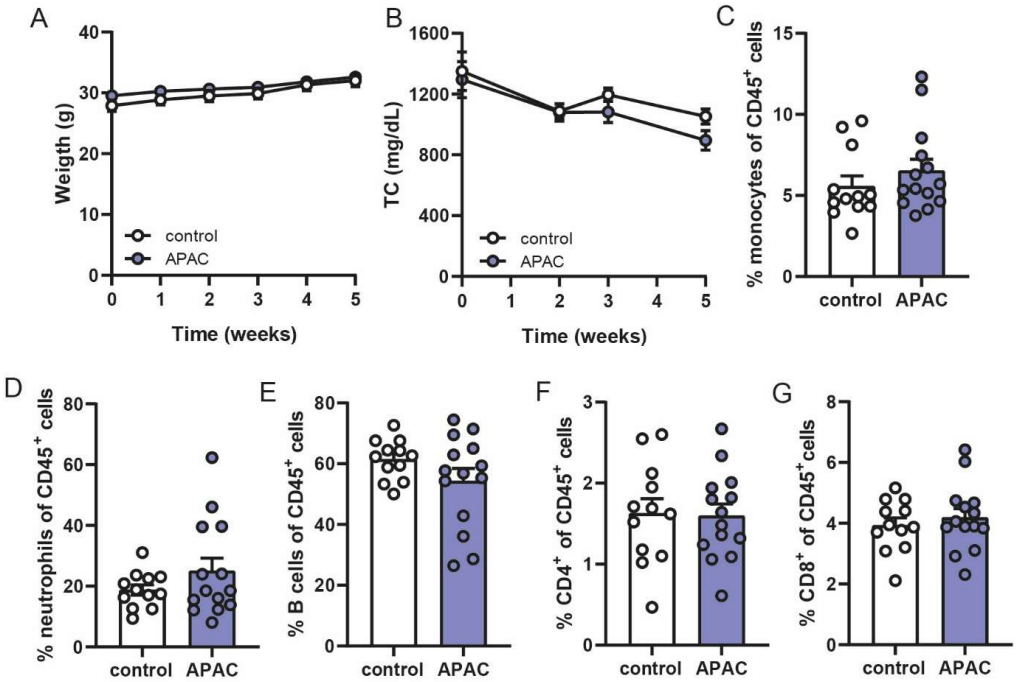

Supplementary figure 3. Systemic effects of APAC administration in the prevention setting. A) Total body weight, and B) plasma cholesterol levels during the study did not differ between the groups. Upon sacrifice, the relative amount of C) $CD11b^{+}Ly6C^{+}$ monocytes and that of D) $CD11b^{+}Ly6G^{+}$ neutrophils did not differ between the groups. Similarly, D) $CD19^{+}$ B cells, E) $CD4^{+}$ T lymphocyte and F) $CD8^{+}$ T lymphocyte levels in the circulation were similar between the groups. N=12-14 per group, data are given as mean±SEM.

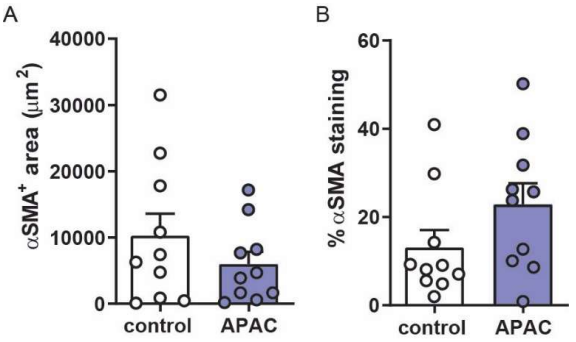

Supplementary figure 4. Smooth muscle cell content in the prevention study. A) Total α-smooth muscle actin (αSMA) surface area and B) αSMA positive area as percentage of total plaque area did not differ between the APAC treated and control group. Data are given as mean±SEM.

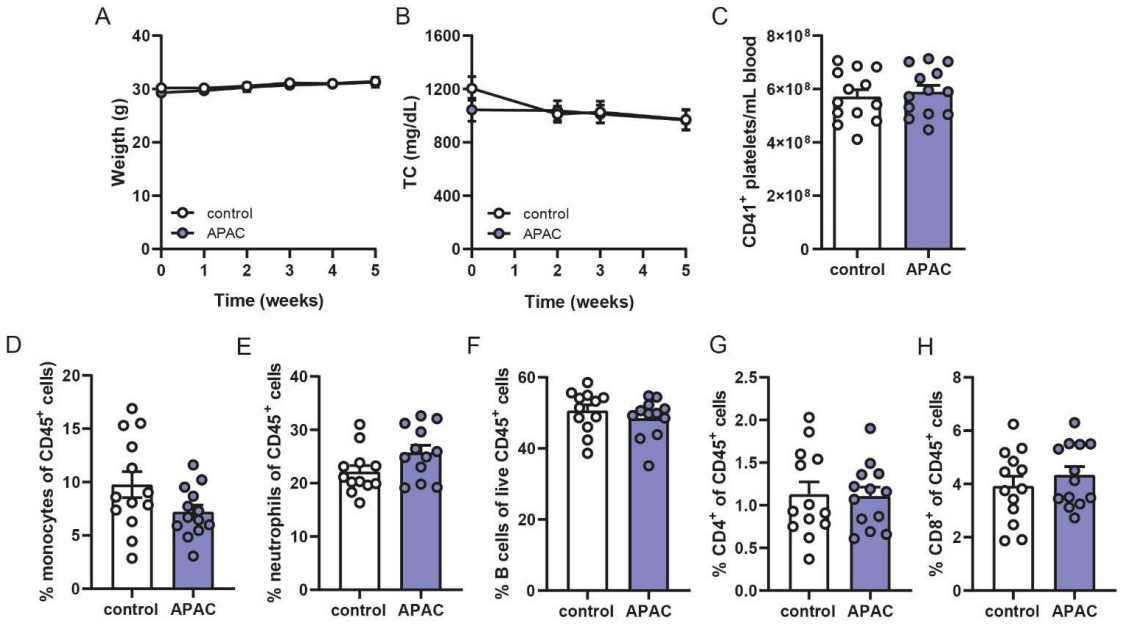

Supplementary figure 5. Systemic effects of APAC in the treatment setting. A) Total body weight and B) plasma total cholesterol (TC) levels were not affected by APAC treatment during the study. Total platelet count (C) and the relative level of D) $CD11b^{+}Ly6C^{+}$ monocytes and E) $CD11b^{+}Ly6G^{+}$ neutrophils were equal in both groups. F) $CD19^{+}$ B lymphocyte, G) $CD4^{+}$, and H) $CD8^{+}$ T lymphocyte levels did not differ between the groups. N=12-14 per group, data are given as mean±SEM.

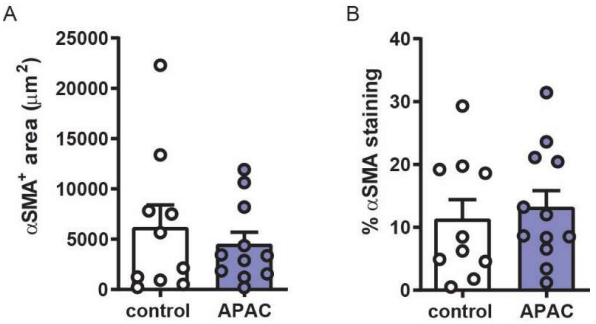

Supplementary figure 6. Smooth muscle cell content in the treatment setting. A) Total αSMA surface area and B) αSMA positive area as percentage of total plaque area did not differ between the APAC treated and control group. Data are given as mean±SEM.